JACS
JOURNAL OF THE AMERICAN CHEMICAL SOCIETY
pubs.acs.org/JACS
Article

Exceptional Nuclease Resistance of Paranemic Crossover (PX) DNA and Crossover-Dependent Biostability of DNA Motifs

Arun Richard Chandrasekaran,* Javier Vilcapoma, Paromita Dey, Siu Wah Wong-Deyrup, Bijan K. Dey, and Ken Halvorsen*

Cite This: https://dx.doi.org/10.1021/jacs.0c02211
Read Online

ABSTRACT: Nanometer-sized features and molecular recognition properties make DNA a useful material for nanoscale construction, but degradation in biological fluids poses a considerable roadblock to biomedical applications of DNA nanotechnology. Here, we report the remarkable biostability of a multistranded motif called paranemic crossover (PX) DNA. Compared to double stranded DNA, PX DNA has dramatically enhanced (sometimes >1000 fold) resistance to degradation by four different nucleases, bovine and human serum, and human urine. We trace the cause of PX's biostability to DNA crossovers, showing a continuum of protection that scales with the number of crossovers. These results suggest that enhanced biostability can be engineered into DNA nanostructures by adopting PX-based architectures or by strategic crossover placement.

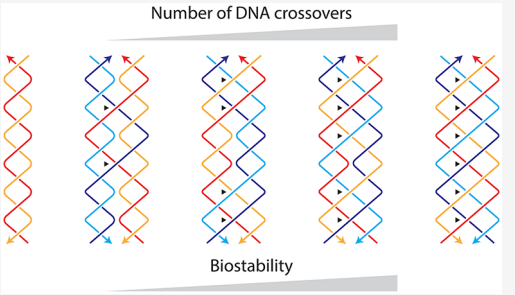

INTRODUCTION

Some daring purveyors of science fiction have imagined superior beings with more than two strands of DNA. In the 1997 movie, *The Fifth Element*, for example, the heroine Leeloo is considered a perfect human-like being in part because of her 8-stranded helical DNA that is "tightly packed with infinite genetic knowledge". While this is notably incorrect, there are instances both in biology and biotechnology where DNA structures can have more than two strands. Triplexes, for example, can form a single helix using three strands,[1] while guanine tetrads can form four-stranded DNA complexes.[2]

For DNA-based nanoscale assembly, synthetic DNA strands are designed and integrated together to form different motifs that serve as the building blocks for bottom-up construction.[3] These (usually) multistranded structures typically contain double helical domains that are connected together by strand crossovers. A wide variety of structures have been made using bottom-up DNA construction, ranging from small objects and devices to larger, trigger-responsive "cages" that have emerging applications in drug delivery. To succeed as drug delivery vehicles, DNA objects must overcome a major challenge of surviving harsh *in vivo* environments such as blood.[4] Strategies to improve the biostability of DNA structures include polymer[5] and protein-based[6−8] coating, viral capsid encapsulation,[9] modified nucleotides,[10,11] and cross-linking.[8,12] One possibility that has been largely overlooked is that the inherent design of these DNA nanostructures can be altered to change biostability.

The construction of DNA nanostructures is based on robust starting units. One example is the double crossover (DX) motif that has two adjacent double helices connected by 2 crossover points.[13] Design rules and construction parameters established on such DNA motifs are applied to other strategies and hierarchical assemblies (for example, the multicrossover DNA origami).[14] Another (less common) DNA motif is paranemic crossover (PX) DNA, a four-stranded DNA structure that consists of two adjacent and connected double helical DNA domains (Figure 1a).[15,16] The motif is formed by creating crossovers between strands of the same polarity at every possible point between two side-by-side helices.[16] Each duplex domain of PX DNA contains alternating major (wide) groove or a minor (narrow) groove separation (denoted by W and N, respectively in Figure 1a) flanking the central dyad axis of the structure, with one helical repeat containing a mixture of four half turns. Previous studies have reported PX DNA with different major/minor groove separations (W:N), with the most stable complexes containing 6, 7, or 8 nucleotides in the major groove and 5 nucleotides in the minor groove (PX 6:5, 7:5, and 8:5, respectively).[15,16]

In DNA nanotechnology, PX DNA has been used to construct objects such as an octahedron[17] and a triangle,[18] as

Received: February 25, 2020

https://dx.doi.org/10.1021/jacs.0c02211
J. Am. Chem. Soc. XXXX, XXX, XXX−XXX

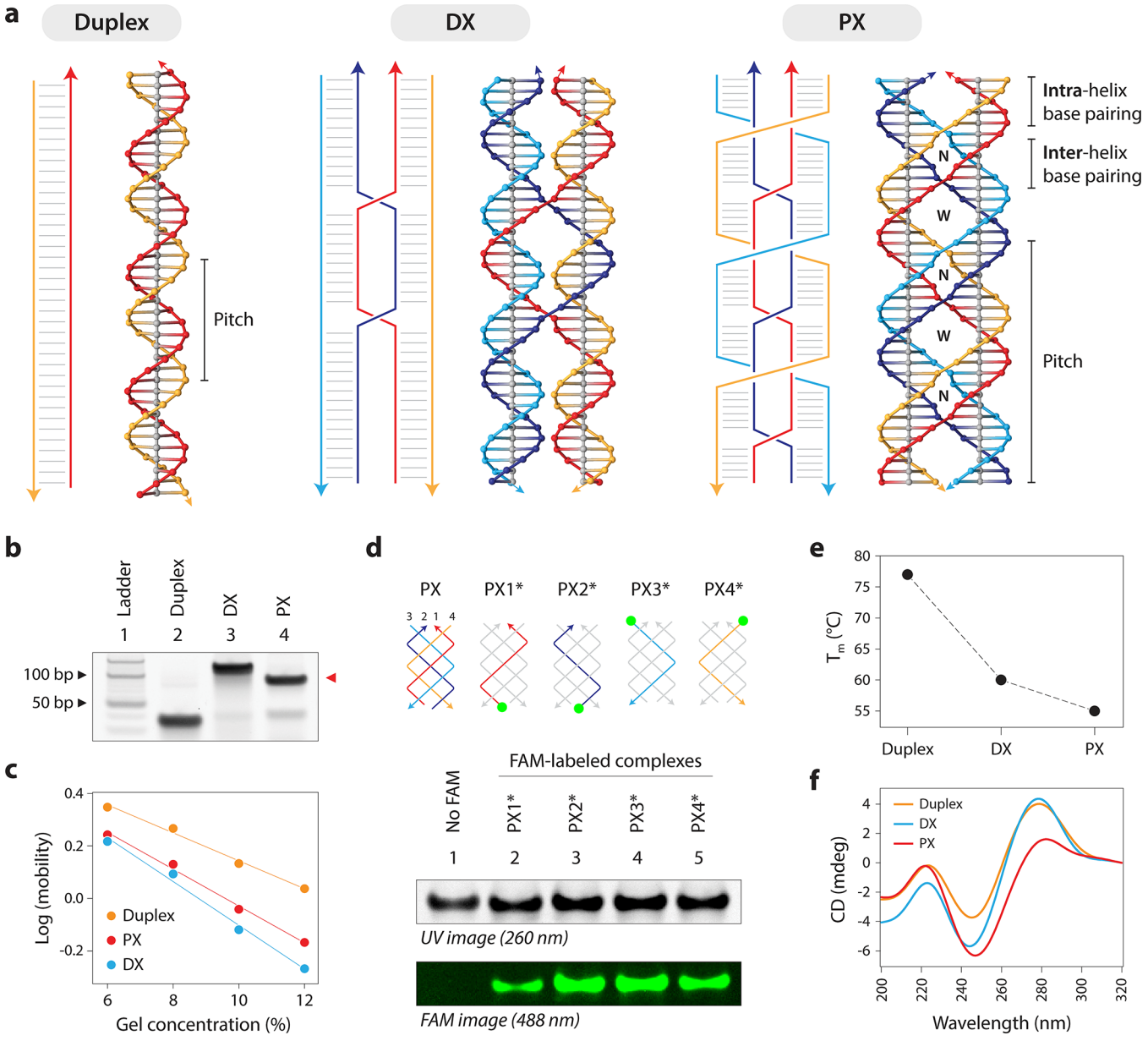

Figure 1. Design and validation of paranemic crossover (PX) DNA. (a) Schematic and molecular models of a B-DNA duplex, a double crossover (DX) motif and paranemic crossover (PX) DNA. (b) Nondenaturing PAGE showing formation of structures as predominant products in each lane, with PX migrating slightly faster than its DX counterpart. (c) Ferguson plot showing gel mobility characteristics of the control and PX structures as a function of gel concentration. (d) Validating incorporation of all four strands in the PX by making four structures each with a single FAM-labeled strand. Gel image under UV is shown for reference, with a control PX lane omitting FAM labels. (e) Melting temperatures determined from UV melting experiment show a decrease in thermal stability from duplex to DX to PX. (f) Circular dichroism spectra of the tested structures show that characteristics of PX is similar to those previously reported.

well as one- and two-dimensional arrays.[19,20] PX DNA has also been a component of nanomechanical devices[21] that are used in molecular assembly lines[22] and DNA-based computation.[23] In biology, PX DNA is studied for its involvement in double stranded DNA homology recognition due to its ability to relax supercoiled DNA.[24] Recent studies sought out proteins in the cell that can structure-specifically bind to PX DNA, so as to elucidate its biological function.[25,26] These studies found that DNA polymerase I (Pol I) and T7 endonuclease I can bind to PX DNA, supporting the notion of its biological relevance. Despite the interest in PX DNA in nanotechnology and biological contexts, the biostability of the structure has not yet been explored.

In this work, we discovered that PX DNA has a remarkable ability to resist nuclease degradation compared to normal DNA duplexes. We show that this increased resistance is varied in magnitude but persistent across multiple enzymes and biological fluids. We find that PX DNA appears almost indestructible to a few nucleases and can withstand 3 biological fluids for 24 h with no evidence of damage. Exploring the cause of this enhanced stability, we find a clear dependence on the number of crossovers, with each additional crossover conferring additional protection. The results suggest that enhanced biostability can be designed into DNA nanostructures.

https://dx.doi.org/10.1021/jacs.0c02211
J. Am. Chem. Soc. XXXX, XXX, XXX−XXX

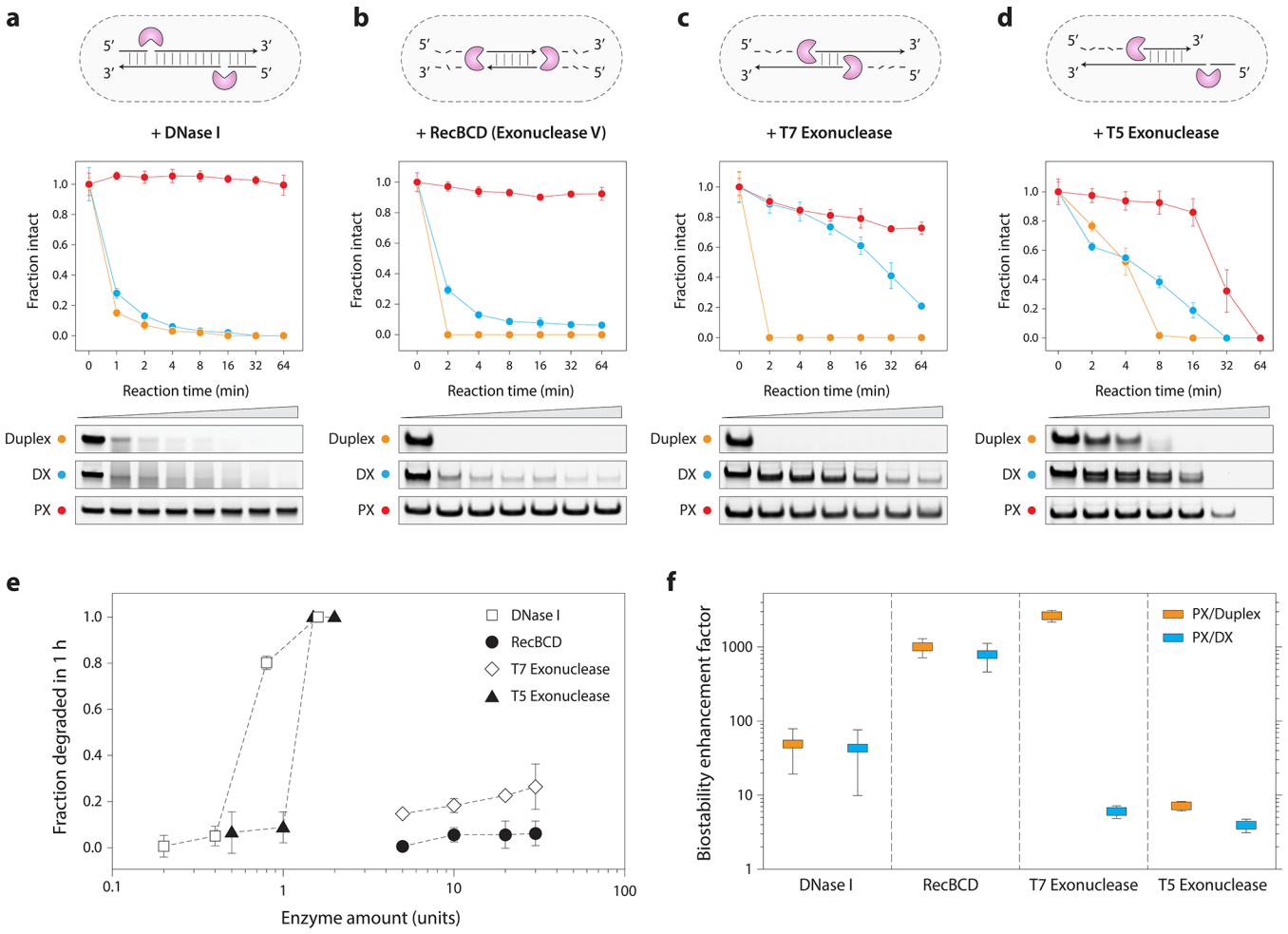

Figure 2. Exceptional nuclease resistance of PX DNA. (a) Degradation of DNA motifs treated with 0.1 unit of DNase I enzyme. (b–d) Degradation of structures treated with RecBCD (exonuclease V), T7 exonuclease, and T5 exonuclease, respectively. The known activity of the tested enzymes on duplex DNA is shown as a cartoon in the corresponding figure panels. (e) Activity of different nucleases on PX DNA. (f) Biostability enhancement factor (fold-increase) of PX DNA as compared to duplex and DX. Error bars are standard deviations calculated from experiments performed in triplicates.

RESULTS

Design and Characterization of PX DNA and Control Structures. In this study, we used a PX 6:5 molecule (6 nucleotides in the major groove and 5 nucleotides in the minor groove),[16,25] where the helical repeat of each strand is 22 nucleotides, making the pitch of the PX DNA roughly twice of that of B-DNA (with a net twist half of that of B-DNA) (Figure 1a, right). We made two control structures: one DNA duplex with the sequence matching half of the PX motif (Figure 1a, left) and a double crossover (DX) motif with sequence similar to the PX but has only two crossover points (Figure 1a, middle). Figure 1 illustrates the crossover points in the strand diagrams for each structure and their respective molecular models (sequences are shown in Figure S1). We annealed the motifs in Tris-acetate-EDTA-Mg^{2+} (TAE) buffer and checked their formation using nondenaturing polyacrylamide gel electrophoresis (PAGE) (Figure 1b and Figure S2). We analyzed the electrophoretic mobility of the different motifs as a function of gel concentration using a Ferguson plot (Figure 1c and Figure S3), where the slope provides an estimate of the retardation (frictional) coefficient of the structures. The plot shows that the slope of the PX molecule is comparable to that of the DX and distinct from a regular double stranded DNA, a trend consistent with previous results.[16] To further confirm the formation of the four-stranded PX, we used fluorescein (FAM)-labeled strands and annealed four different PX complexes each containing one of the FAM-labeled strands (green circles in Figure 1d, labeled strand is indicated by *). The presence of a fluorescent band in each of these four lanes on a nondenaturing PAGE indicated that all four strands are present in the complex (lanes 2–5) compared to a nonlabeled complex (lane 1) (gel image in Figure 1d and Figure S4). We then analyzed the thermal melting profiles of the structures and found that the thermal stability decreases from the duplex (77 °C) to the DX (60 °C) and PX (55 °C) as the number of crossovers increases (Figure 1e and Figure S5). Circular dichroism profiles of the duplex, DX and PX were also consistent with previous reports available for these structures (Figure 1f).[27]

Nuclease Resistance of PX DNA and Control Structures. For the first test of PX DNA biostability, we chose DNase I, one of the most widely used endonucleases in molecular biology that nonspecifically cleaves both strands of double stranded DNA.[28] DNase I performs optimally at the physiological temperature of 37 °C, so we first confirmed that our DNA structures were stable at this temperature for at least

https://dx.doi.org/10.1021/jacs.0c02211
J. Am. Chem. Soc. XXXX, XXX, XXX−XXX

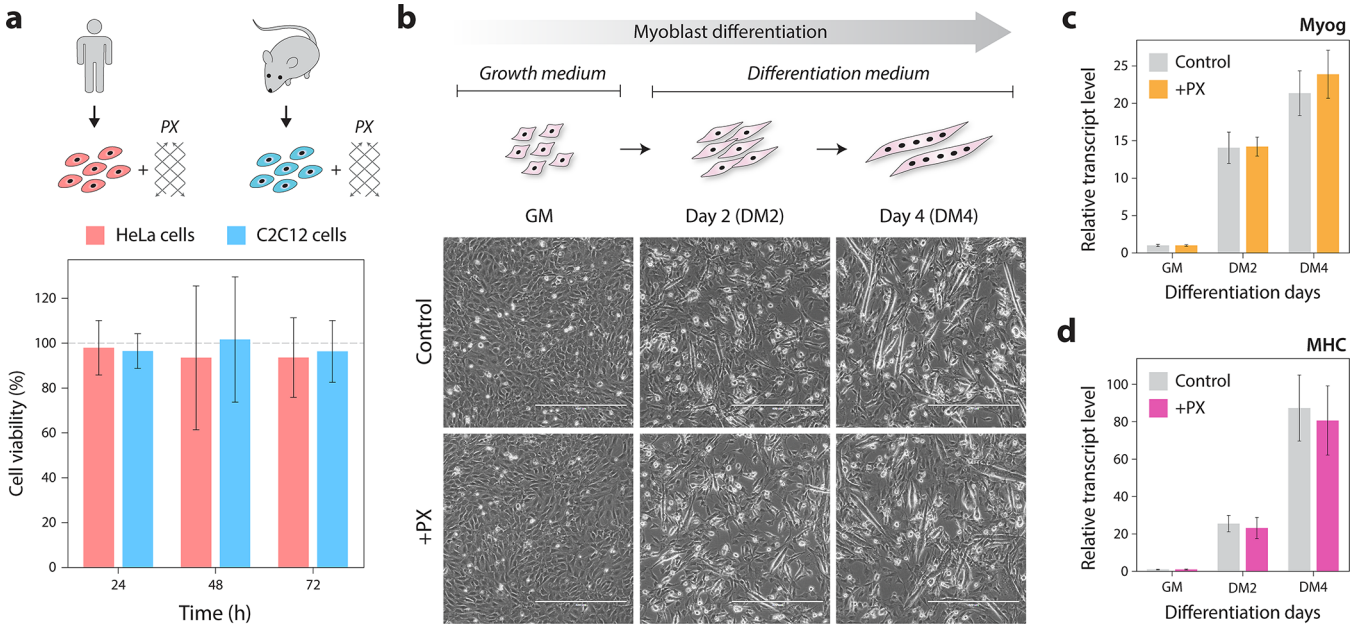

Figure 3. PX DNA does not affect cellular viability or influence cellular differentiation. (a) Cell viability from MTT assay when HeLa cells and C2C12 cells were incubated with 100 nM PX DNA for 24−72 h. Bars represent % of cell viability as compared to the control cells without PX (indicated by gray dashed line). (b) Incubation with PX DNA does not affect differentiation of myoblast cells (C2C12 cell line). Images show undifferentiated (GM), early (DM2) and late (DM4) differentiated cells. Scale bars are 400 μm. (c, d) qRT-PCR results of myogenic differentiation markers Myog and MHC both of which are upregulated in DM2 and DM4 cells in both the control set and cells incubated with PX DNA. The Myog and MHC values are normalized to GM values (as 1) to indicate fold change over time. Values presented are mean ± standard deviation calculated from biological triplicates.

24 h (Figure S6). We probed enzymatic degradation by incubating the PX DNA or relevant controls with DNase I enzyme for different times at 37 °C and quantifying the reduction of the band representing the structure on PAGE gels (Figure 2a and Figures S7 and S8). With 0.1 units of DNase I, the duplex and DX structures were over 90% degraded within a few minutes, while PX DNA had less than 5% degradation even after 1 h. At higher concentrations of DNase I the digestion of all products accelerated but maintained similar trends (Figures S7 and S9).

On the basis of these results, we next tested whether this nuclease resistance of PX holds for nucleases other than DNase I. Since different nucleases can have different activities, mechanisms, substrates, and polarities of digestion, we chose a representative cross section of common nucleases that acts on double stranded DNA. We explored three exonucleases in detail, two with 5′ to 3′ directionality (T7 and T5) and one with bidirectionality (Rec BCD). For all three enzymes, we found that PX was the most stable (Figure 2b−d and Figure S10). We then assessed PX degradation by screening different concentrations of these enzymes. We found that different nucleases had vastly different activity on PX DNA. In a 1 h assay, DNase I and T5 exonuclease fully digested the PX DNA with ∼1 unit enzyme while RecBCD and T7 exonuclease were unable to fully digest the PX even with the highest possible enzyme amounts (30 units) (Figure 2e and Figure S11).

To estimate the biostability enhancement of PX, we identified an optimal concentration for each enzyme to quantify the decay kinetics of PX, DX, and duplex (Figures S12 and S13). We then calculated the fold change in degradation kinetics for PX relative to DX and duplex (Figure 2f). The biostability enhancement factor of PX/duplex ranges from a low of ∼7-fold for T5 exonuclease to a high of ∼2800-fold in T7 exonuclease, with an enhancement of T7 Exo > RecBCD > DNase I > T5 Exo. For PX/DX, the trend was RecBCD > DNase I > T7 exonuclease > T5 exonuclease, with lower enhancement values in general. The data suggests that the enhanced biostability of PX is a somewhat general phenomenon but that certain enzymes struggle more than others with the digestion.

PX DNA Does Not Interfere with Fundamental Biological Processes. The exceptional biostability of PX DNA suggests that the motif may be useful for biological applications of DNA nanotechnology. Considering this important aspect, we asked whether PX DNA interferes with any biological or cellular processes. To address this, we performed cellular viability assay (MTT assay) and cellular differentiation assay (myoblast differentiation assay). We first tested cellular viability in the presence of PX DNA using MTT assays in mouse (C2C12 myoblast) and human (HeLa) cell lines. We incubated the cells either with different concentrations of PX DNA or 1× TAE (control; PX DNA was assembled in 1× TAE) and performed MTT assay (Figure S14). We did not observe any significant changes in cellular viability compared to control cells after 24, 48, and 72 h of incubation with 100 nM PX DNA (Figure 3a).

Next, we examined whether PX DNA affects cellular differentiation using C2C12 myoblast differentiation assays. These cells proliferate in the presence of high serum (Growth Medium; GM) and differentiate in low serum (Differentiation Medium; DM).[29,30] We incubated PX DNA or 1× TAE while culturing the cells either in GM or in DM. We first imaged and later harvested these undifferentiated (GM) and early and late stages of differentiated cells (DM2 and DM4, respectively) for measuring myogenic markers. As shown in the micrographs, PX DNA did not interfere with the normal process of cellular

https://dx.doi.org/10.1021/jacs.0c02211
J. Am. Chem. Soc. XXXX, XXX, XXX−XXX

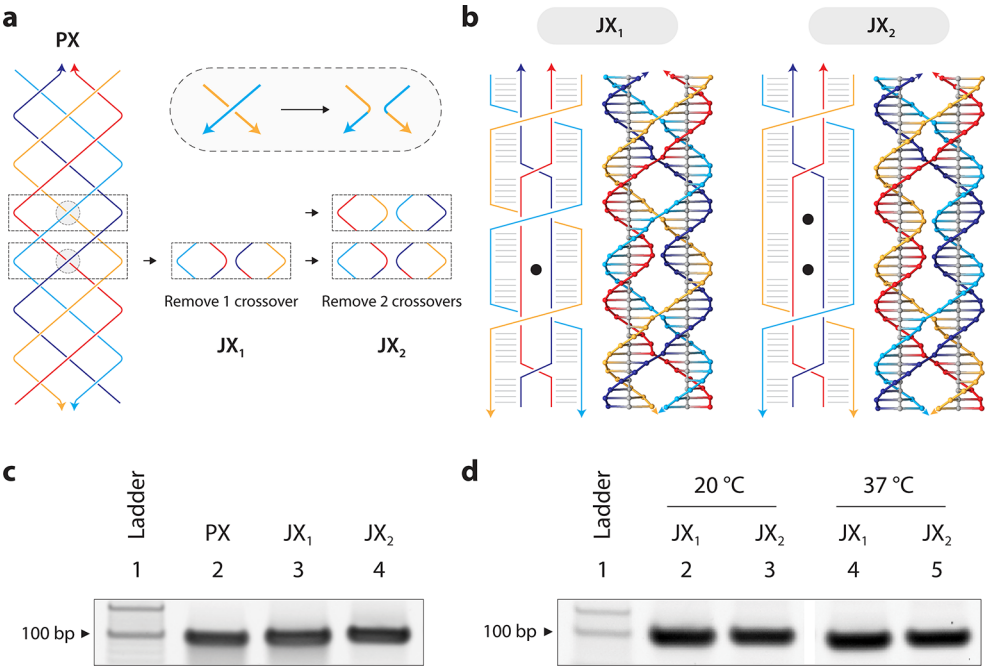

Figure 4. Construction of PX DNA analogs (called JX) with fewer crossovers. (a) Deriving structures with lesser number of crossovers from PX DNA. (b) Schematic and molecular models of JX_1 and JX_2 that lack 1 and 2 crossovers, respectively (shown as black dots in the structural diagram). (c) Nondenaturing PAGE showing formation of JX_1 and JX_2 structures. (d) Stability of JX_1 and JX_2 motifs at 37 °C.

differentiation (Figure 3b). It is apparent from this experiment that PX DNA also did not change the kinetics of differentiation as compared to control (Figure 3b). We further confirmed these findings by quantitating an early myogenic marker, Myogenin (Myog), and a late myogenic marker, Myosin Heavy Chain (MHC), by qRT-PCR analysis. PX DNA did not change the levels of Myog or MHC transcript level (Figure 3c,d). These findings suggest that PX DNA does not affect basic biological or cellular properties and can be used for biological applications in the future.

Removal of Crossovers in PX DNA Reduces Nuclease Resistance. Considering the unusual nuclease resistance of PX DNA, we hypothesized that the nuclease activity may be obstructed by the frequent crossovers in the structure. To test this hypothesis, we constructed variations of the PX DNA motif that have sequentially fewer crossover points, called juxtaposed crossover (JX) DNA motifs (Figure 4a). The JX motifs are denoted with numbers signifying the missing crossovers compared to PX structure (e.g., JX_2 denotes two missing crossovers) (Figure 4b and Figure S15). On the basis of the PX, we designed strands to make JX motifs JX_1, JX_2, and JX_3. Following similar protocols for formation of PX, we formed all three structures (Figure 4c and Figure S16). To our knowledge, the JX_1 and JX_2 structures have been previously demonstrated in the lab,[21,31] while JX_3 has been simulated by molecular dynamics. Simulations predicted these structures to be stable to varying degrees, with a stability trend of PX > JX_1 > JX_2 > JX_3.[32,33] When testing at 37 °C, we found that the JX_1 and JX_2 structures remained stable but not the JX_3; therefore, we omitted this structure from further experiments (Figure 4d and Figure S17). To test the degradation of the JX_1 and JX_2 structures, we incubated them with 0.1 unit DNase I for different time periods (Figure 5a and Figure S18). The results, combined with those showing PX, DX, and duplex, clearly demonstrate that there is a hierarchy of nuclease resistance that follows the trend PX > JX_1 > JX_2 > DX > Duplex. These results support our hypothesis that the nuclease resistance is crossover-dependent.

Enhanced, Crossover Dependent Biostability Is Observed for Multiple Biofluids. The ultimate goal for many practitioners of DNA nanotechnology is to provide solutions to biomedical problems such as drug delivery and biosensing. In such cases, DNA nanostructures may need to survive for hours, days, or weeks in complex biological fluids such as serum or urine. To see if the exceptional and crossover-dependent stability holds for biological fluids, we tested fetal bovine serum (FBS), human serum, and human urine. We incubated each of the five DNA motifs in 10% solutions of these fluids for various time points up to 24 h at 37 °C and analyzed the treated samples on nondenaturing PAGE (Figure 5b–d and Figures S19 and S20). Similar to the nuclease assays, quantified results showed that PX DNA was the most stable in all cases, with no discernible degradation even after 24 h. We also tested the duplex, DX, and PX DNA in different percentages of FBS, and PX was more stable in all cases (Figure S21). The duplex and DX structures were almost completely degraded in the same conditions while the JX structures were again intermediate. From the results of nuclease resistance and biofluids experiments, we did a comparative analysis of all the tested structures to find out the biostability trend as a function of the number of crossovers in the structure (Figure 5e). The overall stability of the structures in all these conditions was PX > JX_1 > JX_2 > DX > duplex (with 6, 5, 4, 2, and 0 crossover points, respectively), reflecting the effect of crossovers on nuclease resistance and biostability.

DISCUSSION

Here, we have discovered that PX DNA has dramatically enhanced biostability compared to normal double stranded DNA that can sometimes exceed 1000-fold. This remarkable difference could have a number of plausible explanations that

https://dx.doi.org/10.1021/jacs.0c02211
J. Am. Chem. Soc. XXXX, XXX, XXX−XXX

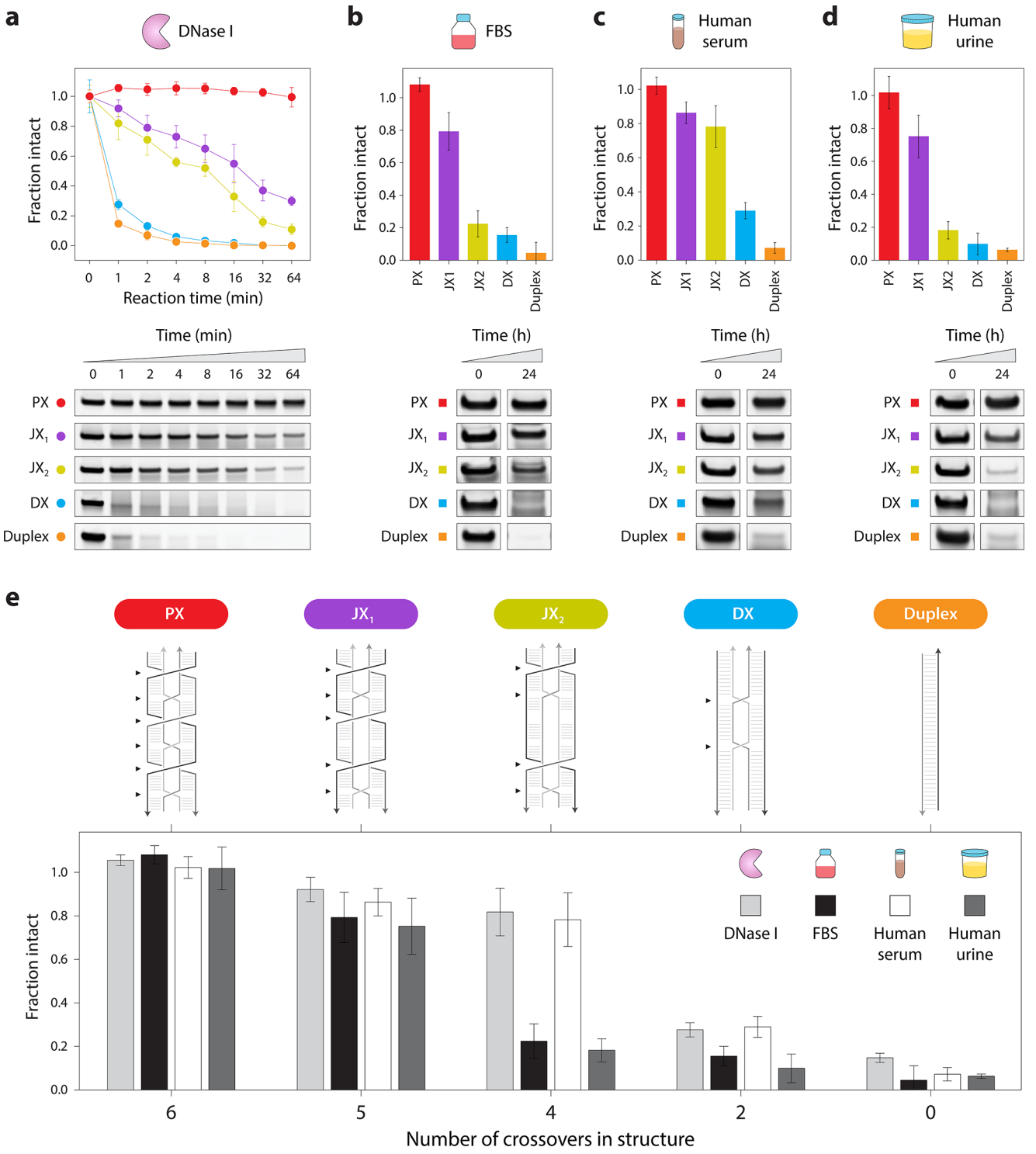

Figure 5. Crossover-dependent biostability. (a) Degradation of PX DNA and control structures when treated with 0.1 unit of DNase I enzyme. (b–d) Nondenaturing gels and degradation plots of control structures (duplex and DX) and PX, JX_1, and JX_2 incubated for 24 h at 37 °C in 10% fetal bovine serum (FBS), human serum, and human urine, respectively. (e) Comparative analysis of the tested structures (PX, JX_1, JX_2, DX, and duplex) in DNase I enzyme (at 1 min reaction time), 10% FBS (at 24 h), 10% human serum (at 24 h), and 10% human urine (at 24 h). Positions of crossovers in each structure are indicated by black arrows. Results show an upward trend in nuclease resistance and biostability with increasing number of crossovers in the structure (PX > JX_1 > JX_2> DX > duplex). Error bars are standard deviations calculated from experiments performed in triplicates.

may merit further study. Enzymatic activity on DNA is known to depend on the helical twist of DNA molecules,[34] with DNase I in particular dependent on groove width and flexibility of the duplex.[35] Thus, the enhanced resistance of PX DNA to DNase I could be in part due to the difference in helical parameters compared to that of regular DNA duplexes. DNase I has also been previously shown to require a substrate of typically 6–8 base pairs,[35,36] and digestion of branched

https://dx.doi.org/10.1021/jacs.0c02211
J. Am. Chem. Soc. XXXX, XXX, XXX−XXX

junctions has shown that several nucleotides near the branch point are protected from DNase I cleavage.[37] In PX DNA, crossovers occur every half turn and thus the available double helical region between consecutive crossovers is only 5 or 6 base pairs (alternating half turns). These small regions may make DNase I binding difficult or impossible and slow the degradation. Our results on the JX motifs are consistent with these possible explanations, as removal of each crossover will both extend potential binding regions and relax the DNA in that region. This explanation might also hold true for the other exonucleases we tested, most of which require flexibility and unwinding of the DNA substrate for processing.[38]

DNA nanostructures have previously been shown to exhibit enhanced nuclease resistance compared to oligonucleotides or plasmid DNA,[39] but stability of DNA nanostructures remains a major problem in the field.[40] Previous studies have shown that DNA nanostructures incubated with 10% FBS degraded within a few hours.[41−43] Some stabilization strategies have been proposed, including heat treatment of FBS,[41] addition of actin protein to inhibit nuclease activity,[41] or chemical modification of component DNA strands.[43] However, these strategies are not without disadvantages. Heat treatment and addition of external proteins can affect the physiological environment and are probably not feasible *in vivo*, while chemically modified nucleic acids can sometimes be toxic or induce unwanted immune responses.

Our findings suggest that PX DNA based nanostructures should be inherently more biostable than typical DNA nanostructures. While direct quantitative comparison against previous studies is difficult, it is worth noting that our PX DNA showed no signs of degradation at 24 h in 10% FBS, while DNA origami objects were largely destroyed under similar conditions.[41] Since DNA nanostructures tend to be more nuclease resistant than their individual structural components, we predict that larger DNA objects constructed from PX motifs will be more enzyme resistant than duplex based nanostructures. A few DNA nanostructures including the recently developed single-stranded origami[44] have utilized PX DNA, but the relative biostability of similar PX and non-PX nanostructures has not yet been investigated to see if our predictions hold true.

Beyond using PX DNA motifs to increase robustness for biological applications of DNA nanostructures, our discovery of crossover-dependent biostability suggests that biostability can be engineered into DNA nanostructures. For example, it could be possible to add protection to structures by strategic placement of crossovers at areas that are especially exposed to nucleases. Such a strategy could lead to DNA nanostructures with a "tunable" biostability dictated by bottom-up design principles. In drug delivery applications, this type of tailored biostability would facilitate timed degradation for fast or slow release of the encapsulated cargo. Further studies in DNA nanostructures containing different number or arrangement of crossovers are certainly needed to see if such speculation is fully grounded in reality. Coming full circle back to our introduction, the sci-fi writers of *The Fifth Element* were not always (or ever) grounded in reality, but they were inadvertently on to something with their idea of enhancement by more than two DNA strands. At least for the 4-stranded PX DNA structure, perhaps enhanced biostability is "the fifth element".

■ ASSOCIATED CONTENT

Supporting Information

The Supporting Information is available free of charge at https://pubs.acs.org/doi/10.1021/jacs.0c02211.

Materials and methods, sequences used, experimental results, and full gel images (PDF)

■ AUTHOR INFORMATION

Corresponding Authors

Arun Richard Chandrasekaran − *The RNA Institute, University at Albany, State University of New York, Albany, New York 12222, United States;* orcid.org/0000-0001-6757-5464; Email: arun@albany.edu

Ken Halvorsen − *The RNA Institute, University at Albany, State University of New York, Albany, New York 12222, United States;* orcid.org/0000-0002-2578-1339; Email: khalvorsen@albany.edu

Authors

Javier Vilcapoma − *The RNA Institute, University at Albany, State University of New York, Albany, New York 12222, United States*

Paromita Dey − *The RNA Institute and Department of Biological Sciences, University at Albany, State University of New York, Albany, New York 12222, United States*

Siu Wah Wong-Deyrup − *The RNA Institute and Department of Biological Sciences, University at Albany, State University of New York, Albany, New York 12222, United States*

Bijan K. Dey − *The RNA Institute and Department of Biological Sciences, University at Albany, State University of New York, Albany, New York 12222, United States*

Complete contact information is available at: https://pubs.acs.org/10.1021/jacs.0c02211

Notes

The authors declare no competing financial interest.

■ ACKNOWLEDGMENTS

Research reported in this publication was supported by the NIH through NIGMS under award R35GM124720 to K.H. and by the American Heart Association under award 17SDG33670339 and NIAMS under award R15AR074728 to B.K.D. We thank Dr. Jibin Abraham Punnoose for discussions on the project, Johnsi Mathivanan for assistance with CD experiments, and Andrew Hayden for the pop-culture reference to multistranded DNA in *The Fifth Element*.

■ REFERENCES

(1) Chandrasekaran, A. R.; Rusling, D. A. Triplex-Forming Oligonucleotides: A Third Strand for DNA Nanotechnology. *Nucleic Acids Res.* **2018**, *46* (3), 1021−1037.

(2) Lipps, H. J.; Rhodes, D. G-Quadruplex Structures: In Vivo Evidence and Function. *Trends Cell Biol.* **2009**, *19* (8), 414−422.

(3) Seeman, N. C.; Sleiman, H. F. DNA Nanotechnology. *Nat. Rev. Mater.* **2018**, *3* (1), 17068.

(4) Madhanagopal, B. R.; Zhang, S.; Demirel, E.; Wady, H.; Chandrasekaran, A. R. DNA Nanocarriers: Programmed to Deliver. *Trends Biochem. Sci.* **2018**, *43* (12), 997−1013.

(5) Agarwal, N. P.; Matthies, M.; Gür, F. N.; Osada, K.; Schmidt, T. L. Block Copolymer Micellization as a Protection Strategy for DNA Origami. *Angew. Chem., Int. Ed.* **2017**, *56* (20), 5460−5464.

(6) Ponnuswamy, N.; Bastings, M. M. C.; Nathwani, B.; Ryu, J. H.; Chou, L. Y. T.; Vinther, M.; Li, W. A.; Anastassacos, F. M.; Mooney,

D. J.; Shih, W. M. Oligolysine-Based Coating Protects DNA Nanostructures from Low-Salt Denaturation and Nuclease Degradation. *Nat. Commun.* **2017**, *8* (1), 1−9.
(7) Auvinen, H.; Zhang, H.; Nonappa Kopilow, A.; Niemelä, E. H.; Nummelin, S.; Correia, A.; Santos, H. A.; Linko, V.; Kostiainen, M. A. Protein Coating of DNA Nanostructures for Enhanced Stability and Immunocompatibility. *Adv. Healthcare Mater.* **2017**, *6* (18), 1700692.
(8) Anastassacos, F. M.; Zhao, Z.; Zeng, Y.; Shih, W. M. Glutaraldehyde Cross-Linking of Oligolysines Coating DNA Origami Greatly Reduces Susceptibility to Nuclease Degradation. *J. Am. Chem. Soc.* **2020**, *142* (7), 3311−3315.
(9) Perrault, S. D.; Shih, W. M. Virus-Inspired Membrane Encapsulation of DNA Nanostructures To Achieve In Vivo Stability. *ACS Nano* **2014**, *8* (5), 5132−5140.
(10) Kim, K.-R.; Kim, H. Y.; Lee, Y.-D.; Ha, J. S.; Kang, J. H.; Jeong, H.; Bang, D.; Ko, Y. T.; Kim, S.; Lee, H.; Ahn, D.-R. Self-Assembled Mirror DNA Nanostructures for Tumor-Specific Delivery of Anticancer Drugs. *J. Controlled Release* **2016**, *243*, 121−131.
(11) Liu, Q.; Liu, G.; Wang, T.; Fu, J.; Li, R.; Song, L.; Wang, Z.-G.; Ding, B.; Chen, F. Enhanced Stability of DNA Nanostructures by Incorporation of Unnatural Base Pairs. *ChemPhysChem* **2017**, *18* (21), 2977−2980.
(12) Cassinelli, V.; Oberleitner, B.; Sobotta, J.; Nickels, P.; Grossi, G.; Kempter, S.; Frischmuth, T.; Liedl, T.; Manetto, A. One-Step Formation of "Chain-Armor"-Stabilized DNA Nanostructures. *Angew. Chem., Int. Ed.* **2015**, *54* (27), 7795−7798.
(13) Fu, T. J.; Seeman, N. C. DNA Double-Crossover Molecules. *Biochemistry* **1993**, *32* (13), 3211−3220.
(14) Rothemund, P. W. K. Folding DNA to Create Nanoscale Shapes and Patterns. *Nature* **2006**, *440* (7082), 297−302.
(15) Wang, X.; Chandrasekaran, A. R.; Shen, Z.; Ohayon, Y. P.; Wang, T.; Kizer, M. E.; Sha, R.; Mao, C.; Yan, H.; Zhang, X.; Liao, S.; Ding, B.; Chakraborty, B.; Jonoska, N.; Niu, D.; Gu, H.; Chao, J.; Gao, X.; Li, Y.; Ciengshin, T.; Seeman, N. C. Paranemic Crossover DNA: There and Back Again. *Chem. Rev.* **2018**, *119* (10), 6273−6289.
(16) Shen, Z.; Yan, H.; Wang, T.; Seeman, N. C. Paranemic Crossover DNA: A Generalized Holliday Structure with Applications in Nanotechnology. *J. Am. Chem. Soc.* **2004**, *126* (6), 1666−1674.
(17) Shih, W. M.; Quispe, J. D.; Joyce, G. F. A 1.7-Kilobase Single-Stranded DNA That Folds into a Nanoscale Octahedron. *Nature* **2004**, *427* (6975), 618.
(18) Liu, W.; Wang, X.; Wang, T.; Sha, R.; Seeman, N. C. PX DNA Triangle Oligomerized Using a Novel Three-Domain Motif. *Nano Lett.* **2008**, *8* (1), 317−322.
(19) Ohayon, Y. P.; Sha, R.; Flint, O.; Liu, W.; Chakraborty, B.; Subramanian, H. K. K.; Zheng, J.; Chandrasekaran, A. R.; Abdallah, H. O.; Wang, X.; Zhang, X.; Seeman, N. C. Covalent Linkage of One-Dimensional DNA Arrays Bonded by Paranemic Cohesion. *ACS Nano* **2015**, *9* (10), 10304−10312.
(20) Shen, W.; Liu, Q.; Ding, B.; Shen, Z.; Zhu, C.; Mao, C. The Study of the Paranemic Crossover (PX) Motif in the Context of Self-Assembly of DNA 2D Crystals. *Org. Biomol. Chem.* **2016**, *14* (30), 7187−7190.
(21) Yan, H.; Zhang, X.; Shen, Z.; Seeman, N. C. A Robust DNA Mechanical Device Controlled by Hybridization Topology. *Nature* **2002**, *415* (6867), 62.
(22) Gu, H.; Chao, J.; Xiao, S.-J.; Seeman, N. C. A Proximity-Based Programmable DNA Nanoscale Assembly Line. *Nature* **2010**, *465* (7295), 202−205.
(23) Chakraborty, B.; Jonoska, N.; Seeman, N. C. A Programmable Transducer Self-Assembled from DNA. *Chem. Sci.* **2012**, *3* (1), 168−176.
(24) Wang, X.; Zhang, X.; Mao, C.; Seeman, N. C. Double-Stranded DNA Homology Produces a Physical Signature. *Proc. Natl. Acad. Sci. U. S. A.* **2010**, *107* (28), 12547−12552.
(25) Gao, X.; Gethers, M.; Han, S.; Goddard, W. A.; Sha, R.; Cunningham, R. P.; Seeman, N. C. The PX Motif of DNA Binds Specifically to Escherichia Coli DNA Polymerase I. *Biochemistry* **2019**, *58* (6), 575−581.
(26) Kizer, M.; Huntress, I. D.; Walcott, B. D.; Fraser, K.; Bystroff, C.; Wang, X. Complex between a Multicrossover DNA Nanostructure, PX-DNA, and T7 Endonuclease I. *Biochemistry* **2019**, *58* (10), 1332−1342.
(27) Niu, D.; Jiang, H.; Sha, R.; Canary, J. W.; Seeman, N. C. The Unusual and Dynamic Character of PX-DNA. *Nucleic Acids Res.* **2015**, *43* (15), 7201−7206.
(28) Laskowski, M. 12 Deoxyribonuclease I. In *The Enzymes*; Boyer, P. D., Ed.; Hydrolysis; Academic Press: 1971; Vol. *4*, pp 289−311. DOI: 10.1016/S1874-6047(08)60372-8.
(29) Dey, B. K.; Gagan, J.; Dutta, A. miR-206 and -486 induce myoblast differentiation by downregulating Pax7. *Mol. Cell. Biol.* **2011**, *31* (1), 203−214.
(30) Dey, B. K.; Gagan, J.; Yan, Z.; Dutta, A. miR-26a is required for skeletal muscle differentiation and regeneration in mice. *Genes Dev.* **2012**, *26* (19), 2180−2191.
(31) Spink, C. H.; Ding, L.; Yang, Q.; Sheardy, R. D.; Seeman, N. C. Thermodynamics of Forming a Parallel DNA Crossover. *Biophys. J.* **2009**, *97* (2), 528−538.
(32) Maiti, P. K.; Pascal, T. A.; Vaidehi, N.; Goddard, W. A. The Stability of Seeman JX DNA Topoisomers of Paranemic Crossover (PX) Molecules as a Function of Crossover Number. *Nucleic Acids Res.* **2004**, *32* (20), 6047−6056.
(33) Santosh, M.; Maiti, P. K. Structural Rigidity of Paranemic Crossover and Juxtapose DNA Nanostructures. *Biophys. J.* **2011**, *101* (6), 1393−1402.
(34) Lomonossoff, G. P.; Butler, P. J. G.; Klug, A. Sequence-Dependent Variation in the Conformation of DNA. *J. Mol. Biol.* **1981**, *149* (4), 745−760.
(35) Weston, S. A.; Lahm, A.; Suck, D. X-Ray Structure of the DNase I-d(GGTATACC)2 Complex at 2·3Å Resolution. *J. Mol. Biol.* **1992**, *226* (4), 1237−1256.
(36) Suck, D. DNA Recognition by DNase I. *J. Mol. Recognit.* **1994**, *7* (2), 65−70.
(37) Lu, M.; Guo, Q.; Seeman, N. C.; Kallenbach, N. R. DNase I Cleavage of Branched DNA Molecules. *J. Biol. Chem.* **1989**, *264* (35), 20851−20854.
(38) Ceska, T. A.; Sayers, J. R. Structure-Specific DNA Cleavage by 5′ Nucleases. *Trends Biochem. Sci.* **1998**, *23* (9), 331−336.
(39) Keum, J.-W.; Bermudez, H. Enhanced Resistance of DNA nanostructures to Enzymatic Digestion. *Chem. Commun.* **2009**, No. 45, 7036−7038.
(40) Stephanopoulos, N. Strategies for Stabilizing DNA Nanostructures to Biological Conditions. *ChemBioChem* **2019**, *20* (17), 2191−2197.
(41) Hahn, J.; Wickham, S. F. J.; Shih, W. M.; Perrault, S. D. Addressing the Instability of DNA Nanostructures in Tissue Culture. *ACS Nano* **2014**, *8* (9), 8765−8775.
(42) Mei, Q.; Wei, X.; Su, F.; Liu, Y.; Youngbull, C.; Johnson, R.; Lindsay, S.; Yan, H.; Meldrum, D. Stability of DNA Origami Nanoarrays in Cell Lysate. *Nano Lett.* **2011**, *11* (4), 1477−1482.
(43) Conway, J. W.; McLaughlin, C. K.; Castor, K. J.; Sleiman, H. DNA Nanostructure Serum Stability: Greater than the Sum of Its Parts. *Chem. Commun.* **2013**, *49* (12), 1172−1174.
(44) Han, D.; Qi, X.; Myhrvold, C.; Wang, B.; Dai, M.; Jiang, S.; Bates, M.; Liu, Y.; An, B.; Zhang, F.; Yan, H.; Yin, P. Single-Stranded DNA and RNA Origami. *Science* **2017**, *358* (6369), No. eaao2648.

https://dx.doi.org/10.1021/jacs.0c02211
J. Am. Chem. Soc. XXXX, XXX, XXX−XXX